European Journal of Pharmaceutical Sciences 170 (2022) 106113

Contents lists available at ScienceDirect

European Journal of Pharmaceutical Sciences

journal homepage: www.elsevier.com/locate/ejps

Electrospun poly(ω-pentadecalactone-*co*-ε-caprolactone)/gelatin/chitosan ternary nanofibers with antibacterial activity for treatment of skin infections

Cansu Ulker Turan *, Yuksel Guvenilir

Istanbul Technical University, Department of Chemical Engineering, Istanbul, Turkey

ARTICLE INFO

Keywords:
Electrospinning
Tetracycline hydrochloride
Drug delivery
Gelatin
Chitosan
ω-pentadecalactone
ε-caprolactone

ABSTRACT

In recent years, there is an increasing attention on biocompatible electrospun nanofibers for drug delivery applications since they provide high surface area, controlled and sustained drug release, and they mimic the extracellular matrix. In the present study, tetracycline hydrochloride (TCH) antibiotic loaded poly(ω-pentadecalactone-*co*-ε-caprolactone)/gelatin/chitosan nanofibrous membranes were fabricated as a controlled drug delivery system. Poly(ω-pentadecalactone-*co*-ε-caprolactone) copolymer has been enzymatically synthesized in previous studies, thus it provides an originality to the membrane. Combination of a synthetic polymer, a protein, and a polysaccharide in order to obtain a synergetic effect is another novelty of this work and there exists limited examples for such electrospun membrane. Varied amounts of TCH was electrospun together with poly(ω-pentadecalactone-*co*-ε-caprolactone)/gelatin/chitosan (50/40/10 vol ratio) polymer blend (fiber diameters ranged between 85.7–225.2 nm) and several characterizations (morphological and molecular structure, wettability characteristics, and thermal behavior) were applied to examine the drug incorporation. Subsequently, *in vitro* drug release studies were conducted and mathematical modeling was applied for the detection of transport mechanism of drug. TCH release proceeded 14 days through an initial burst release in first hour and followed by a sustained release. 1% TCH-loaded sample was shown as optimal preparation with 96.5% total drug release and 11.8% initial burst release. TCH-loaded preparations demonstrated a good antibacterial activity against Gram-positive (*Staphylococcus aureus* and *Bacillus subtilis*) bacteria and a limited effect (no inhibition zone observed below 3% TCH concentration) against Gram-negative (*Escherichia coli*) bacterium. Thus, TCH concentrations of ≥ 3% could be preferred to obtain a wide-spectrum effectiveness. The presented drug delivery system is suggested to be applied for treatment of skin infections as a wound dressing device.

1. Introduction

Controlled drug delivery systems (DDS) have been developed to safely transport the drugs to a target site in the body and improve the therapeutic effects (Basar et al., 2017; Ghafoor et al., 2018; Li et al., 2019; Martínez-Pérez, 2020; Moydeen et al., 2018). In conventional drug treatment methods, drug circulates through the whole blood system by spreading to also healthy areas and rapidly removed from the body which necessitates the intake of an extra amount of drug or multiple dosing to achieve the required therapy (Basar et al., 2017; Ghafoor et al., 2018; Li et al., 2019; Martínez-Pérez, 2020; Moydeen et al., 2018). This situation leads to several drawbacks such as toxicity, undesired side effects, and drug level fluctuations in plasma (Basar et al., 2017; Ghafoor et al., 2018; Kumar and Domb, 2008; Laha et al., 2016). Recently, there is an increasing interest on fabrication of polymer-based DDS which are capable of providing a controlled delivery of drug to a targeted site and sustained release (Basar et al., 2017; Kumar and Domb, 2008; Madhaiyan et al., 2013). Polymer films, gels, particulates prepared via spray drying, emulsion technique or freeze spray atomization, and nanofibers obtained via electrospinning have been reported for the fabrication of polymer-based DDS (Basar et al., 2017; Canbolat et al., 2014; Ghafoor et al., 2018; Kumar and Domb, 2008). Among these methods, electrospinning is a frequently used versatile drug encapsulation method, in which ultrathin polymer fibers are fabricated under high voltage (Basar et al., 2017; Ghafoor et al., 2018; Kajdič et al., 2019; Luraghi et al., 2021). Moreover, by the encapsulation of therapeutic

* Corresponding author.
E-mail address: ulkerc@itu.edu.tr (C. Ulker Turan).

https://doi.org/10.1016/j.ejps.2021.106113
Received 15 September 2021; Received in revised form 8 December 2021; Accepted 30 December 2021
Available online 2 January 2022

agent via electrospinning, some crucial drawbacks encountered in other DDS fabrication methods, including low encapsulation efficiency and uncontrolled drug release, can be prevented by enabling a good control over drug release and high drug encapsulation efficiency due to high surface to volume ratio and porosity of nanofibers (Allafchian et al., 2020; Basar et al., 2017; Ghafoor et al., 2018; Kajdič et al., 2019; Moydeen et al., 2018; Topuz and Uyar, 2019). Additionally, electrospun nanofibers mimic the structure and function of extracellular matrix (ECM), which promotes site-specific delivery, cell attachment and proliferation. These features make them advantageous for biomedical applications such as tissue engineering and wound healing (Chen et al., 2018; Ghafoor et al., 2018; Kersani et al., 2020; Luraghi et al., 2021; Martínez-Pérez, 2020; Qasim et al., 2018; Sridhar et al., 2015; Ye et al., 2019).

Nanofibrous DDS can be used for transportation of numerous active ingredients (*e.g.* antibiotics, antimyocits, analgesics, anti-cancer drugs, non-steroidal anti-inflammatory drugs, growth factors, and nucleic acids) via different delivery routes such as oral, oromucosal, and transdermal (Chen et al., 2018; Kajdič et al., 2019; Pelipenko et al., 2015; Sofi et al., 2020; Torres-Martinez et al., 2018) For the production of nanofibrous drug carriers, various natural (*e.g.* chitosan, gelatin, collagen, silk sericin) and synthetic (*e.g.* poly(vinyl alcohol), poly (ethylene oxide), poly(ε-caprolactone), poly(lactic acid)) polymers can be utilized depending on the desired final product features, such as drug release mechanism, polymer-drug interactions, mechanical properties, and antibacterial activity (El-Okaily et al., 2021; Pelipenko et al., 2015; Sridhar et al., 2015; Torres-Martinez et al., 2018). Based on the application area, therapeutic agents can be loaded into electrospun nanofibers via encapsulation, embedding, or coating, by the utilization of different type of electrospinning methods (*e.g.* coaxial, emulsion, traditional/direct electrospinning) (Ghafoor et al., 2018; Kersani et al., 2020; Moydeen et al., 2018; Ye et al., 2019). Among the electrospinning methods, traditional electrospinning is the simplest method, in which polymers are directly dissolved in solvent system prior to electrospinning. Drug molecule can be incorporated either by dissolving together with the polymers before electrospinning or by embedding after nanofiber production (Ye et al., 2019).

Skin is one of the crucial organs, since it plays role on keeping the internal fluid homeostasis and providing barrier against chemical, mechanical, and radiological damages (Ghorbani et al., 2020; He et al., 2020). Thus, injury of skin could be considered as an important health problem. Although skin has the ability of self-regeneration, wound healing may be delayed due to infections and require the application of antibiotics (Ghorbani et al., 2020). Tetracycline hydrochloride (TCH) is a widely used antibiotic for treatment of bacterial infections of the skin, which may be resulted from a cut, burn, or surgical operation (Alavarse et al., 2017; Chong et al., 2015; Haroosh et al., 2014; Karuppuswamy et al., 2015) TCH can be applied in wound healing applications by incorporation into a nanofibrous membrane made of biocompatible polymers, which may accelerate regeneration of fibroblasts (Ghorbani et al., 2020; Karuppuswamy et al., 2015; Ulker Turan et al., 2021).

In the present study, TCH-loaded poly(ω-pentadecalactone-*co*-ε-caprolactone)/gelatin/chitosan nanofibers were developed. It was aimed to design a multi-functional drug delivery device by combining a synthetic polymer, a protein, and a polysaccharide. There exist only a few studies that fabricated electrospun nanofibers from triple blends, since optimization and stabilization of electrospinning process becomes difficult as the polymer solution gets complicated. Poly(ω-pentadecalactone-*co*-ε-caprolactone) is a hydrophobic, semi-crystalline, and biocompatible copolymer which was previously synthesized via lipase immobilized onto rice husk ashes (Ulker and Guvenilir, 2018). Enzymatically synthesized polymers have been rarely applied for the fabrication of electrospun nanofibrous DDS, due to their low molecular weights which makes difficult to collect fibers properly. However, in biomedical applications, enzymatically synthesized polymer may be more advantageous than a polymer synthesized by organometallic catalysts, since there would be no residual metal in the product, which may enhance the biocompatibility and reduce the cytotoxicity (Albertsson and Srivastava, 2008; Li et al., 2020, 2011; Liu et al., 2020). Enzymatically synthesized poly(ω-pentadecalactone-*co*-ε-caprolactone) copolymer was expected to avoid uncontrolled water uptake due to its hydrophobicity and provide well-defined degradation and mechanical properties to the nanofibrous DDS (Bhatia, 2016; Kim and Kim, 2014). Gelatin (Gel) is a water-soluble natural polymer, which is derived from the hydrolysis of collagen and extensively preferred for biomedical applications (*e.g.* drug delivery, wound healing, and tissue engineering) due to its nontoxic, non-carcinogenic, biocompatible, and biodegradable nature (Akhmetova and Heinz, 2021; Aldana and Abraham, 2017; Bangar et al., 2014; Huang et al., 2018; Juncos Bombin et al., 2020; Khatti et al., 2017; Pereira et al., 2014; Samrot et al., 2020; Sridhar et al., 2015). Besides, gelatin is known to be easily accepted by the body without immunogenicity, to promote cell proliferation, and to provide site-specific drug transportation due to its functional groups (Akhmetova and Heinz, 2021; Bangar et al., 2014; Basar et al., 2017; Huang et al., 2018; Khatti et al., 2017; Samrot et al., 2020). It was aimed to benefit from these features by the participation of gelatin in prepared electrospun DDS. Chitosan (CS) is a positively charged polysaccharide biopolymer and obtained by partial deacetylation of chitin. Outstanding specialties, such as biodegradability, biocompatibility, antimicrobial activity, cell adhesion properties, and non-toxicity make chitosan favorable for biomedical uses. Especially for wound healing applications, the capability of interaction with negatively charged ECM due to its positively charged amino groups is an attractive feature, which promotes cell adhesion and proliferation. However, electrospinning of chitosan is a challenging issue due to its poor solubility in common organic solvents, high crystallinity and viscosity. By blending with poly (ω-pentadecalactone-*co*-ε-caprolactone) and gelatin, spinnability of chitosan was purposed to be enhanced (Augustine et al., 2020; Azmana et al., 2021; El-Okaily et al., 2021; Qasim et al., 2018).

The main purpose of this work is fabrication of a TCH-loaded nanofibrous wound dressing composed of a triple polymer blend, which combines the advantages of natural and synthetic polymers, for treatment of skin infections. Thus, morphological and molecular structure, wettability characteristics, thermal behavior, TCH release kinetics, and antibacterial activity of the prepared nanofibers have been investigated.

2. Materials and methods

2.1. Materials

Poly(ω-pentadecalactone-*co*-ε-caprolactone) copolymer (M_n=20,960 g/mol) was enzymatically synthesized via ring opening polymerization of equal feed weight ratio of ω-pentadecalactone and ε-caprolactone (Ulker and Guvenilir, 2018). Gelatin from bovine and medium molecular weight chitosan were purchased from Alfasol and Sigma Aldrich, respectively. 1, 1,1,3,3,3-hexafluoroisopropanol (HFIP) solvent (Jinan Finer Chemical Co.) and formic acid (Merck) were used for preparation of electrospinning solutions. Tetracycline hydrochloride (TCH) was supplied from Sigma Aldrich. 25% aqueous solution of glutaraldehyde (Merck) was applied for cross-linking of nanofibrous membranes. Sodium chloride (Carlo Erba), potassium chloride (Merck), disodium hydrogen phosphate dihydrate (J. T. Baker), and potassium dihydrogen phosphate (Carlo Erba) were used for the preparation of pH 7.4 phosphate buffer saline. For the microbiological studies, Nutrient Broth, Agar-agar, and Mueller-Hinton Agar were used to prepare growth media and purchased from Sigma-Aldrich. *Staphylococcus aureus* (ATCC 6538), *Bacillus subtilis* (ATCC 6633), and *Escherichia coli* (ATCC 8739) bacteria were obtained from Istanbul Technical University Food Engineering Department. All chemicals and reagents were of analytical grade.

2.2. Fabrication of neat and drug-loaded electrospun copolymer/gelatin/chitosan nanofibrous membranes

Chitosan (CS) solution (1 wt.%) was prepared in HFIP/Formic acid (2:1, v/v) solvent system by stirring for 48 h at 40 °C. Copolymer (Cop) was dissolved in HFIP and stirred for 24 h at room temperature to obtain 15 wt.% solution. Gelatin (Gel) solution (8 wt.%) was prepared in HFIP by stirring at 40 °C for 2 h. Finally, copolymer, gelatin, and chitosan solutions were mixed in volume ratio of (Cop/Gel/Cs) 50/50/0, 50/40/10, and 50/30/20, respectively and stirred for an hour. Obtained blends were loaded into 5 ml syringes that connected to a metallic nozzle (0.8 mm inner diameter) via polyethylene tubing (2 mm inner diameter) and delivered by a syringe pump fixed at 1.5–2 ml/h flow rate. Electrospinning was carried out at 23–25 kV applied voltage and 17 cm tip-to-collector distance. .

For the preparation of drug-loaded electrospun Cop/Gel/Cs nanofibrous membranes, calculated amount of TCH was dissolved in HFIP together with copolymer by arranging the amount of drug to be 0.5, 1, 3, and 5% (w/v) of total polymer concentration in the final Cop/Gel/Cs blend with 50/40/10 vol ratio. Other procedures for preparation of solutions were applied in a similar manner with the first case. Varied amounts of drug including polymer solutions were electrospun with 2 ml/h flow rate, 25 kV applied voltage, and 17 cm tip-to-collector distance.

All electrospinning experiments were conducted on a Nanospinner 24 Touch (Inovenso) electrospinning device at ambient conditions.

2.3. Cross-linking

Since both nanofibrous gelatin and chitosan are water-soluble and mechanically weak natural polymers, their application areas may be limited (Chen et al., 2017; Schiffman and Schauer, 2007; Zhang et al., 2006). In this study, electrospun Cop/Gel/Cs nanofibrous membranes were utilized in drug delivery and expected to be durable at least until the whole drug is released. Therefore, cross-linking was applied to nanofibrous membranes (~0.1 mm thick) after drying in vacuum oven at 30 °C for 24 h. Cross-linking was performed in a desiccator containing 10 ml 25% aqueous glutaraldehyde in a petri dish. Nanofibrous membranes were cross-linked under glutaraldehyde vapor at 25 °C for 2 h and dried at 80 °C for 2 h to remove residual glutaraldehyde (Zhang et al., 2006).

2.4. In vitro degradation test

Neat and cross-linked Cop/Gel/Cs nanofibrous membranes were cut into a size of 1 × 1 cm^2 and placed in 10 ml pH 7.4 PBS solution. Samples were incubated in a shaking water bath (120 rpm) at 37 °C for 4 weeks. At the end of pre-determined degradation periods, samples were filtered from degradation medium, washed with distilled water, and dried in oven over night at 37 °C. Weight loss was calculated using Eq. (1).

$$Weight\ loss\ (\%) = \frac{W_0 - W_t}{W_0}\ x\ 100 \quad (1)$$

Where W_0 is the initial weight and W_t is the dry weight at any time (Ahmed et al., 2016).

2.5. In vitro drug release

Cross-linked and TCH-loaded Cop/Gel/Cs nanofibrous membranes (3 replicates for each drug loading ratio) were cut into a size of 2 × 2 cm^2 and weighed. All preparations were soaked into 10 ml of pH 7.4 phosphate buffered saline (PBS) and put into shaking water bath (120 rpm) at 37 °C (Alavarse et al., 2017; Basar et al., 2017; Yang et al., 2019). Aliquots of 1 ml were removed and replaced with fresh PBS at specified time periods. Absorbance of removed aliquots were measured by using UV spectrophotometer (UV mini 1240 SHIMADZU) at 343 nm. Amount of released drug was defined according to a predetermined calibration graph and cumulative drug release percentage was calculated using Eq. (2) (Karuppuswamy et al., 2015; Ulker Turan et al., 2021).

$$\text{Cumulative drug release } (\%) = \frac{\text{Total amount of drug released } (\mu g)}{\text{Initial amount of drug present } (\mu g)} \times 100 \quad (2)$$

2.6. Mathematical modeling of drug release data

Four mathematical equations (zero order, first order, Higuchi, and Korsmeyer-Peppas) were used for the analysis of TCH release from Cop/Gel/Cs nanofibrous membranes (Baishya, 2017). Applied kinetic models were explained with following equations (Baishya, 2017; Pisani et al., 2019). The best fitted mathematical model was chosen based on the highest correlation coefficient (R^2) obtained by linear regression analysis.

$$Q = Q_0 + K_0 t \quad (3)$$

Where Q_0 is the initial concentration of drug, K_0 is the zero-order rate constant, and t is the time.

$$\log Q = \log Q_0 - K_1\ t/2.303 \quad (4)$$

Where K_1 is the first order rate constant ($time^{-1}$).

$$Q = K_H\ t^{0.5} \quad (5)$$

Where K_H is the Higuchi constant which indicates the design variables of the system ($time^{-0.5}$). This model assumes that the rate limiting step is Fickian diffusion (Saurí et al., 2014).

$$Q = K_{KP}\ t^n \quad (6)$$

Where K_{KP} is the Korsmeyer-Peppas release rate constant and n is release exponent, which depends on the type of transport, geometry, and polydispersity of solute. This model represents diffusion-controlled drug release (Baishya, 2017).

Depending on the release exponent, diffusional release mechanisms were classified as; $n<0.5$ pseudo-Fickian diffusional behavior, $n = 0.5$ Fickian diffusion, $0.5<n<1$ non-Fickian diffusion, $n = 1$ case II transport (zero order release), and $n>1$ super case II transport (Grkovic et al., 2017).

2.7. Antibacterial activity test

Antibacterial activities of cross-linked and TCH-loaded Cop/Gel/Cs nanofibrous membranes against Gram-positive (*Staphylococcus aureus* and *Bacillus subtilis*) and Gram-negative bacteria (*E. coli*) were determined by the application of disk diffusion method (Hudzicki, 2016). Neat Cop/Gel and Cop/Gel/Cs nanofibrous membranes were used as control samples. Samples with varied amounts of TCH (3 replicates for each) and control samples were cut into 6-mm diameter disks. Bacteria were incubated in Nutrient Broth at 37 °C for 24 h and turbidity of 0.5 McFarland (Biosan Den-1 densitometer) was arranged prior to application to obtain a concentration of 10^8 CFU/ml for each type of bacteria. Mueller-Hinton Agar plates were inoculated with 100 μL of each bacterial suspension by spread plate method. Control samples and three replicates of TCH-loaded Cop/Gel/Cs nanofibrous membranes were placed on the plates and incubated at 37 °C for 24 h. Inhibition zones were measured at the end of incubation period.

2.8. Scanning electron microscopy (SEM)

Surface morphology of the samples were observed by using a scanning electron microscope (SEM, TESCAN VEGA 3) operated at 15 kV.

Before the analysis, samples were coated with Au/Pd by using a SC7620 sputter coater (Quorum Technologies Ltd, UK). Diameters of 100 fibers in each SEM image were measured by applying Image J software. For the analysis of fiber diameter distribution Origin 9.0 software was used.

2.9. Water contact angle measurement

Contact angles of samples were measured using Attension (KSV) equipment. Water droplets were deposited from a syringe on the surfaces of samples. Static water contact angles were calculated via equipment software. Each sample was measured five times.

2.10. Spectroscopic characterization

Energy-dispersive X-Ray spectrometer (EDS) connected to SEM was used to evaluate the composition of nanofibers.

Fourier transform infrared spectroscopy (FTIR) analysis was applied on a Perkin Elmer spectrophotometer in order to define the chemical structure of the samples. Each sample was analyzed by KBr pellet. The spectra were recorded by at least 32 scans with a resolution of 2 cm^{-1}.

2.11. Thermal characterization

Thermal properties were determined by differential scanning calorimetry (DSC) using a TA instruments Q10 calorimeter. Samples were analyzed under inert nitrogen atmosphere at a 50 ml min^{-1} flow rate. Sample scans were carried out between −80 and 250 °C at 10 °C min^{-1} with heat-cool-heat thermal cycles.

Thermal gravimetric analysis (TGA) was applied on a Linseis L81 apparatus for thermal characterization of the samples. The samples were heated from 30 to 550 °C at a heating rate of 10 °C min^{-1} under nitrogen flow.

2.12. Statistical analysis

Three samples were used for each set of drug release experiments. Error bars in the graphs were given as the average ± standard deviation. Minitab 17 software was used for statistical comparisons and analysis of the averages via one-way ANOVA test followed by Tukey test.

3. Results and discussion

3.1. Surface morphology of electrospun cop/gel/cs nanofibrous membranes

Copolymer/gelatin/chitosan (Cop/Gel/Cs) triple blends were prepared by keeping copolymer composition constant as 50% (v/v) of polymer blend based on our previous study in which binary blend of copolymer/gelatin with equal volume ratios resulted in successful nanofibrous structure (Ulker Turan and Guvenilir, 2021).

Chitosan compositions in triple blends were adjusted as 0% (binary blend of copolymer and gelatin), 10%, and 20% in volumetric basis. SEM images obtained from electrospinning of these three samples were shown in Fig. 1 together with distribution histograms which were close to normal distribution (Fig. 1(g)). Increasing the chitosan composition resulted in thinner nanofibers (56.8 ± 22.1 nm for 20% chitosan ratio), however bead formation was observed between nanofibers which may be due to high viscosity of polymer blend solution (Sill and von Recum, 2008). Bead formation was eliminated by decreasing chitosan ratio to 10% (Fig. 1(b)). When compared with nanofibers obtained from binary blend of copolymer and gelatin which was produced in previous study (Fig. 1(a)), significantly lower average diameter (239.3 ± 126.8 nm) was observed by participation of 10% chitosan ($p<0.001$) (Ulker Turan and Guvenilir, 2021). Reduction in fiber diameter by the addition or ratio increment of chitosan may be due to its polycationic nature that enhances charge density and conductivity of the polymer jet (Alavarse

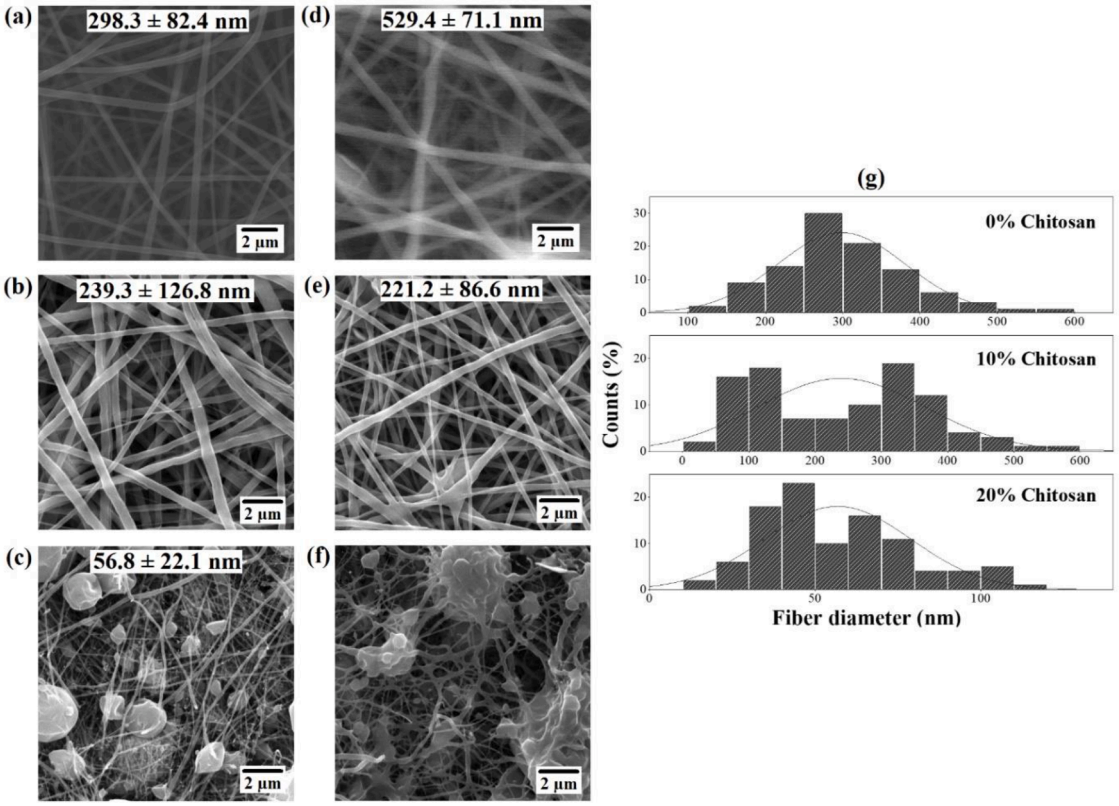

Fig. 1. (a) 0% (Ulker Turan and Guvenilir, 2021), (b) 10%, (c) 20% chitosan, cross-linked (d) 0% (Ulker Turan and Guvenilir, 2021), (e) 10%, (f) 20% chitosan, (g) fiber diameter distribution of nanofibrous membranes without cross-linking.

et al., 2017; Van Der Schueren et al., 2012). Obtained nanofibers with considerably small diameters will be advantageous for drug loading and release which may enhance drug diffusion (Ahmed et al., 2016).

Water solubility and mechanical weakness of gelatin and chitosan limits their application areas (Chen et al., 2017; Schiffman and Schauer, 2007; Zhang et al., 2006). In this study, nanofibrous membrane obtained from triple blend of copolymer, gelatin, and chitosan was utilized for drug delivery. For a sustained drug release and efficient medication, drug carrier material should be durable at least until drug release is completed. Therefore, cross-linking via glutaraldehyde vapor was applied in order to increase water resistance, thermal, and mechanical performance (Chen et al., 2017; Schiffman and Schauer, 2007; Zhang et al., 2006). SEM images of cross-linked preparations were also shown in Fig. 1. As seen from Fig. 1(e), nanofibrous structure of 10% chitosan including cop/gel/cs blend was preserved after cross-linking without any significant diameter difference ($p>0.05$).

In order to prove the water resistance of cross-linked Cop/Gel/Cs nanofibers, *in vitro* degradation test was applied and degradation behaviors of neat and cross-linked samples (10% chitosan including preparations) were compared. At the end of 4 weeks, only 18.3% weight loss was calculated for cross-linked sample, whereas neat Cop/Gel/Cs sample lost 92.5% of its initial weight (Fig. 2). These results showed that, cross-linked Cop/Gel/Cs nanofibers may be a good candidate for long term drug delivery applications, since its material integrity was preserved in simulated body fluid.

3.2. Surface morphology of TCH-loaded of electrospun cop/gel/cs nanofibrous membranes

SEM images of TCH-loaded Cop/Gel/Cs nanofibers before and after cross-linking were presented including distribution histograms in Fig. 3. All preparations exhibited smooth, beadless and randomly aligned nanofibers with normally distributed fiber diameters. TCH loading substantially reduced the fiber diameters, which may be a result of enhancement in electrical conductivity of polymer solution (Fig. 1(b) and Fig. 3(a-d)). As reported in many studies, addition of a drug or an ionic salt alters charge density on the ejected polymer jet surface (Haroosh et al., 2014; Kim et al., 2004; Luong-Van et al., 2006; Radisavljevic et al., 2018; Zamani et al., 2010). TCH-loaded Cop/Gel/Cs nanofibers were ultrafine, the diameters were ranged between 85.7 nm and 225.2 nm and tended to increase proportional to TCH loading ratios. However, there were no significant difference between fiber diameters of 3% and 5% TCH-loaded samples ($p>0.05$). After cross-linking, samples preserved their nanofibrous structure and there was no significant diameter increase ($p>0.05$) except 0.5% TCH-loaded sample. Low average diameters of TCH-loaded Cop/Gel/Cs nanofibers provide high surface area to volume ratios which may promote drug release by enhancing mass transfer.

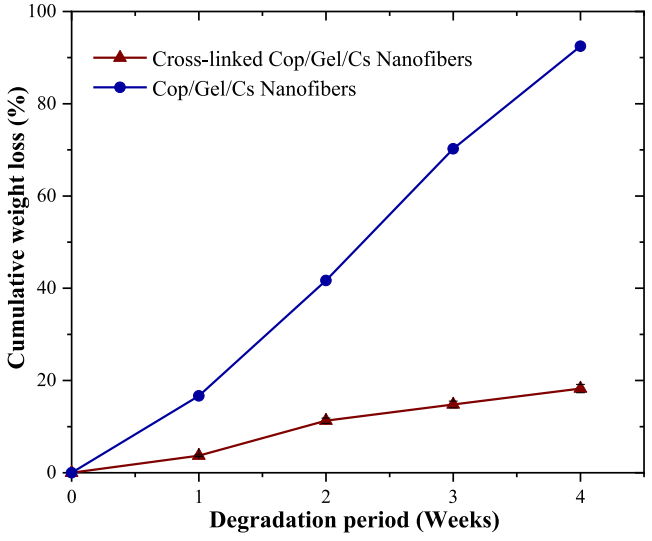

Fig. 2. *In vitro* degradation curves of neat and cross-linked Cop/Gel/Cs nanofibrous membranes.

3.3. In vitro drug release

In vitro drug release behavior of TCH-loaded Cop/Gel/Cs nanofibers (cross-linked) was investigated and cumulative drug release profiles for each preparation were shown in Fig. 4. Drug release profiles were identical with an initial fast release followed by a sustained release until 14th day. It is apparent from Table 1 that, all preparations showed a limited initial burst release (less than 15%) within 1 h which is an extremely important characteristic for controlled drug delivery. It is already known that, drug release from electrospun membranes of hydrophilic polymers (gelatin and chitosan) is generally fast. By blending with a hydrophobic polymer, in this case poly(ω-pentadecalactone-*co*-ε-caprolactone), and application of a proper cross-linking method to further increase the water resistance, it is possible to control the fast release and extend release period (Basar et al., 2017; Chen et al., 2017; Eskitoros-Togay et al., 2019; Schiffman and Schauer, 2007; Zhang et al., 2006).

Total drug release percentages increased inversely proportional to both drug loading ratios and average fiber diameters (Table 1 and Fig. 3) and highest total drug release percentage ($97.2 \pm 0.5\%$) was reached at 0.5% drug loading ratio. However, there were no significant difference between the total drug release ratios of 0.5% and 1% TCH-loaded preparations ($p>0.05$). Since initial burst release of 1% TCH-loaded sample was lower ($11.8 \pm 0.9\%$), this sample could be accepted as the optimum preparation.

As expected, cumulative drug release percentages were higher for nanofibrous membranes with thinner fibers due to high surface area that provides better drug diffusion.

When compared with the previous study which covers fabrication and characterization of TCH-loaded Cop/Gel nanofibrous membranes, drug release amounts were considerably enhanced after addition of chitosan to the polymer blend as a result of achievement of thinner nanofibers (Ulker Turan et al., 2021).

Samples were dried and characterized for morphological changes at the end of 14-days drug release. Both nanofibrous structures seemed to be slightly swelled (fiber diameters were increased) due to contact with PBS solution and regularly disrupted as a result of uniform drug loading and release (Fig. 5). In accordance with *in vitro* degradation experiments, drug-loaded samples seemed to preserve their material integrity and nanofibrous structure at the end of 14-days release period.

3.4. Mathematical modeling of drug release data

In vitro drug release data of each drug loading ratio were fitted to zero order, first order, Higuchi, and Korsmeyer-Peppas mathematical models and all models were applied to analyze first 60% of the release profiles as suggested in literature (Peppas, 1985). Table 2 presents intercepts, slopes, and correlation coefficients (R^2) attained from linearized plots. Higher correlation coefficients ($R^2 > 0.96$) were achieved by the application of Higuchi and Korsmeyer-Peppas models which indicates that TCH release from copolymer/gelatin/chitosan nanofibrous membranes were diffusion-controlled. Best fitted model to *in vitro* drug release profiles was Korsmeyer-Peppas ($R^2 \sim 0.98$–0.99) that specifies the type of diffusion based on release exponent (n) obtained as slope from linearization of Eq. (6) (Baishya, 2017; Pisani et al., 2019; Saurí et al., 2014; Shah and Khan, 2012).

The Korsmeyer-Peppas release exponent (n) values were less than 0.5 (between 0.236 and 0.268) for all preparations which revealed that TCH release mechanism from copolymer/gelatin/chitosan nanofibrous membranes was pseudo-Fickian type diffusion (Grkovic et al., 2017;

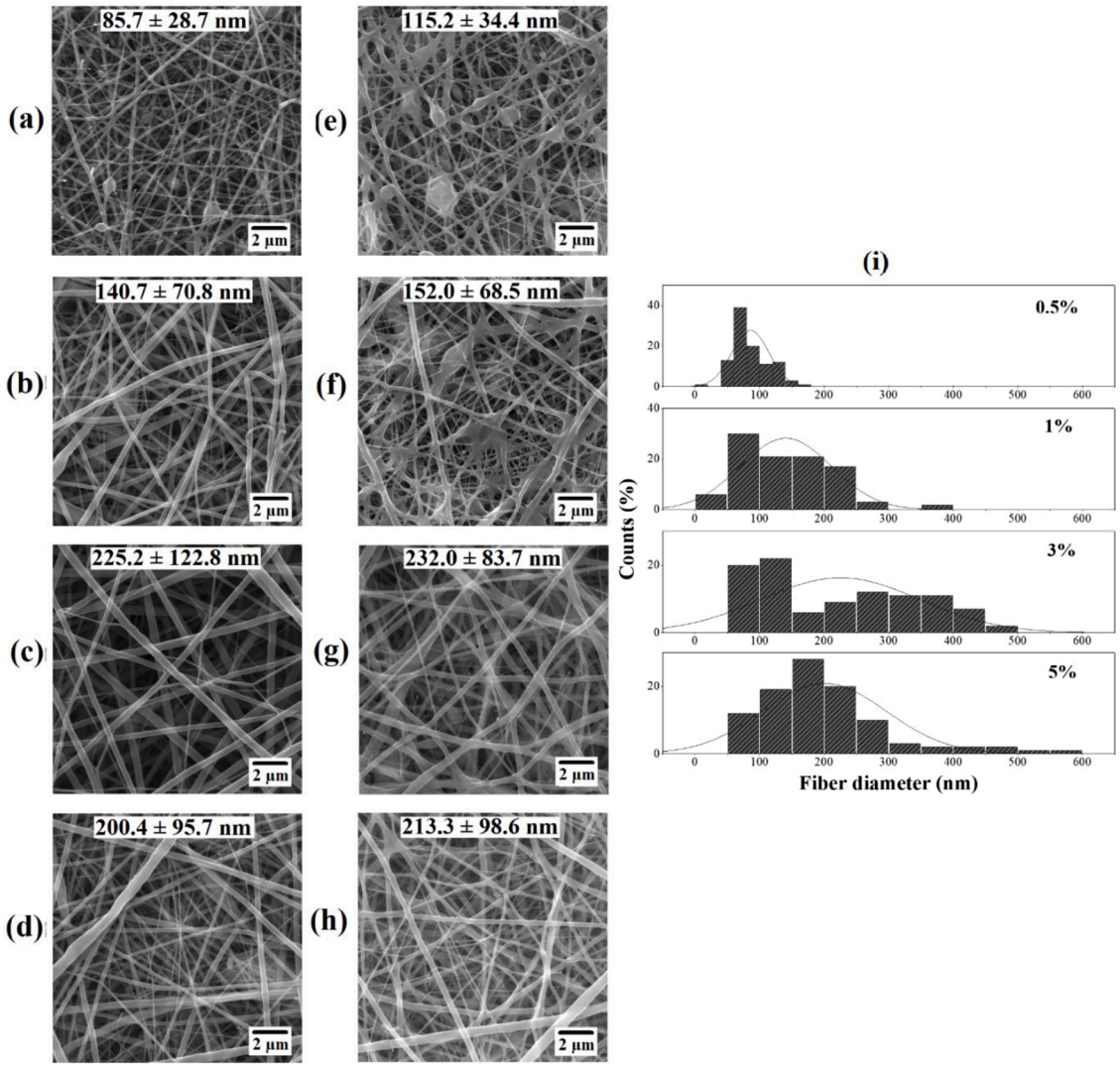

Fig. 3. (a) 0.5%, (b) 1%, (c) 3%, (d) 5%, cross-linked (e) 0.5%, (f) 1%, (g) 3%, (h) 5% TCH-loaded Cop/Gel/Cs nanofibrous membranes, (i) fiber diameter distribution of TCH-loaded nanofibrous membranes without cross-linking.

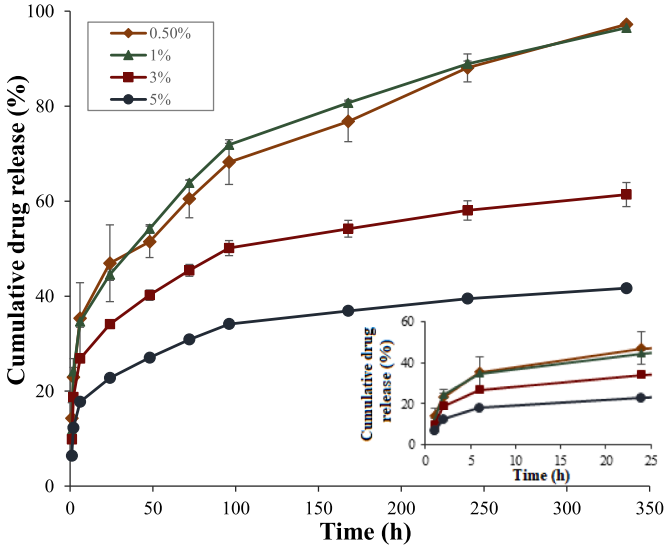

Fig. 4. Drug release profile of Cop/Gel/Cs nanofibrous membranes loaded with varied TCH concentrations.

Table 1
Results for TCH release.

Amount of drug (%)	Burst release within 1h (%)	Total drug release (%)
0.5	14.3 ± 3.3	97.2 ± 0.5
1	11.8 ± 0.9	96.5 ± 0.3
3	9.8 ± 0.3	61.4 ± 2.5
5	6.4 ± 0.1	41.7 ± 0.5

Pisani et al., 2019).

Korsmeyer-Peppas intercept values were assigned to logarithm of release rate constant, K_{KP} (h^{-n}), and as presented in Table 2, fastest drug release was obtained for 0.5% and 1% TCH-loaded preparations.

3.5. Water contact angle measurement

Since electrospun Cop/Gel/Cs nanofibrous membranes were fabricated to be used in drug delivery, at which contact with body fluids is crucial, their wettability characteristics is an important property and investigated via water contact angle measurement. Fig. 6 presents water contact angle measurement results of neat and 1% TCH-loaded membranes with and without cross-linking treatment. As shown in previous studies, poly(ω-pentadecalactone-*co*-ε-caprolactone) was hydrophobic

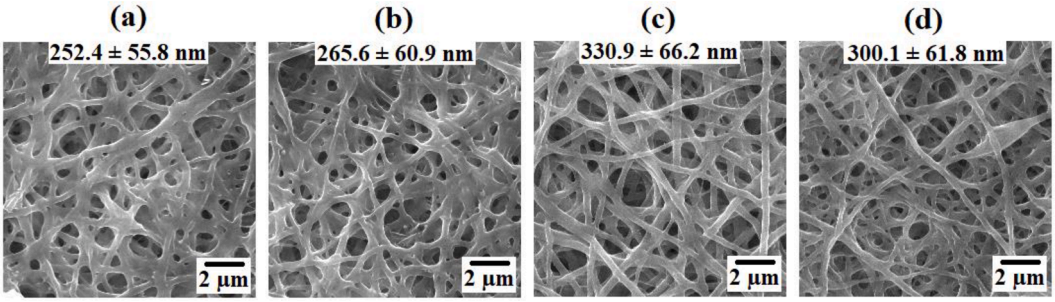

Fig. 5. SEM images obtained at the end of 14-days drug release: (a) 0.5%, (b) 1%, (c) 3%, (d) 5% TCH loading.

Table 2
Values obtained from application of kinetic models to TCH release profiles.

Amount of drug (%)	0.5			1			3			5		
Models	**Intercept**	**Slope**	R^2	**Intercept**	**Slope**	R^2	**Intercept**	**Slope**	R^2	**Intercept**	**Slope**	R^2
Zero order	32.53	0.285	0.8642	34.90	0.332	0.8836	26.07	0.192	0.8298	17.77	0.138	0.8324
First order	3.47	0.006	0.7288	3.55	0.006	0.7679	3.25	0.005	0.7192	2.86	0.006	0.7200
Higuchi	20.39	4.340	0.9724	20.95	5.023	0.9836	17.59	2.969	0.9636	11.68	2.131	0.9649
Korsmeyer-Peppas	1.28	0.262	0.9843	1.32	0.268	0.9890	1.21	0.236	0.9906	1.03	0.245	0.9909

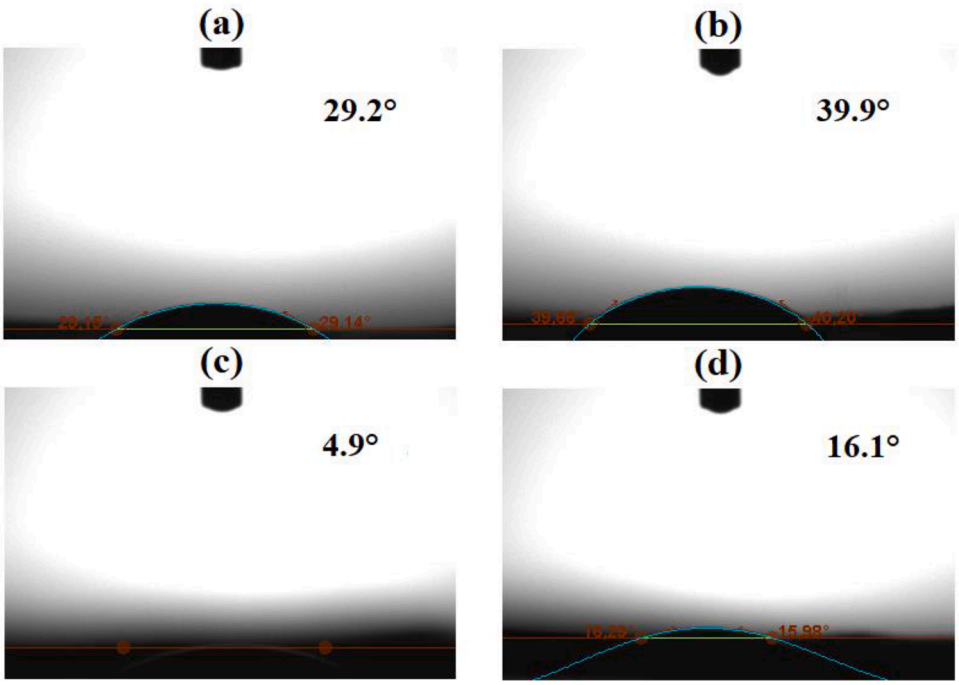

Fig. 6. Water contact angle measurement results: **(a)** Cop/Gel/Cs, **(b)** Cross-linked Cop/Gel/Cs, **(c)**1% TCH-loaded Cop/Gel/Cs, **(d)** Cross-linked 1% TCH-loaded Cop/Gel/Cs nanofibrous membranes.

and addition of gelatin resulted in dramatic decrease in contact angle due to hydrophilic nature of gelatin (Ulker Turan and Guvenilir, 2021). Similarly, chitosan is a hydrophilic natural polymer therefore triple electrospun blend of copolymer, gelatin, and chitosan gave rise to a highly hydrophilic membrane that needed to be cross-linked in order to increase its water resistance. As seen from Fig. 6(b), contact angle increased after cross-linking, in accordance with *in vitro* degradation results, but still low enough which may provide good wettability.

TCH is a hydrophilic drug, therefore contact angle of drug-loaded Cop/Gel/Cs membrane was extremely low (Fig. 6(c)). By the cross-linking treatment, contact angle slightly increased but still less than 90° (Fig. 6(d)). However, as presented in drug release part, cross-linked drug-loaded membranes were durable at the end of 14-days release (Fig. 5) which indicated their hydrolytic resistance. This type of wettability characteristics provides better contact area with body fluids, which is required for a successful mass transfer, so the drug delivery and release would be improved.

3.6. Spectroscopic characterization

FTIR spectra of TCH, copolymer, gelatin, chitosan, Cop/Gel/Cs, cross-linked Cop/Gel, cross-linked neat and 1% TCH-loaded Cop/Gel/Cs nanofibers were compared in Fig. 7. The main bands identifiable to poly (ω-pentadecalactone-*co*-ε-caprolactone) due to asymmetric and symmetric CH_2 stretching (2918 cm^{-1} and 2847 cm^{-1}), carbonyl (C = O) stretching (1720 cm^{-1}), C—O and C—C bonds in the crystalline phase

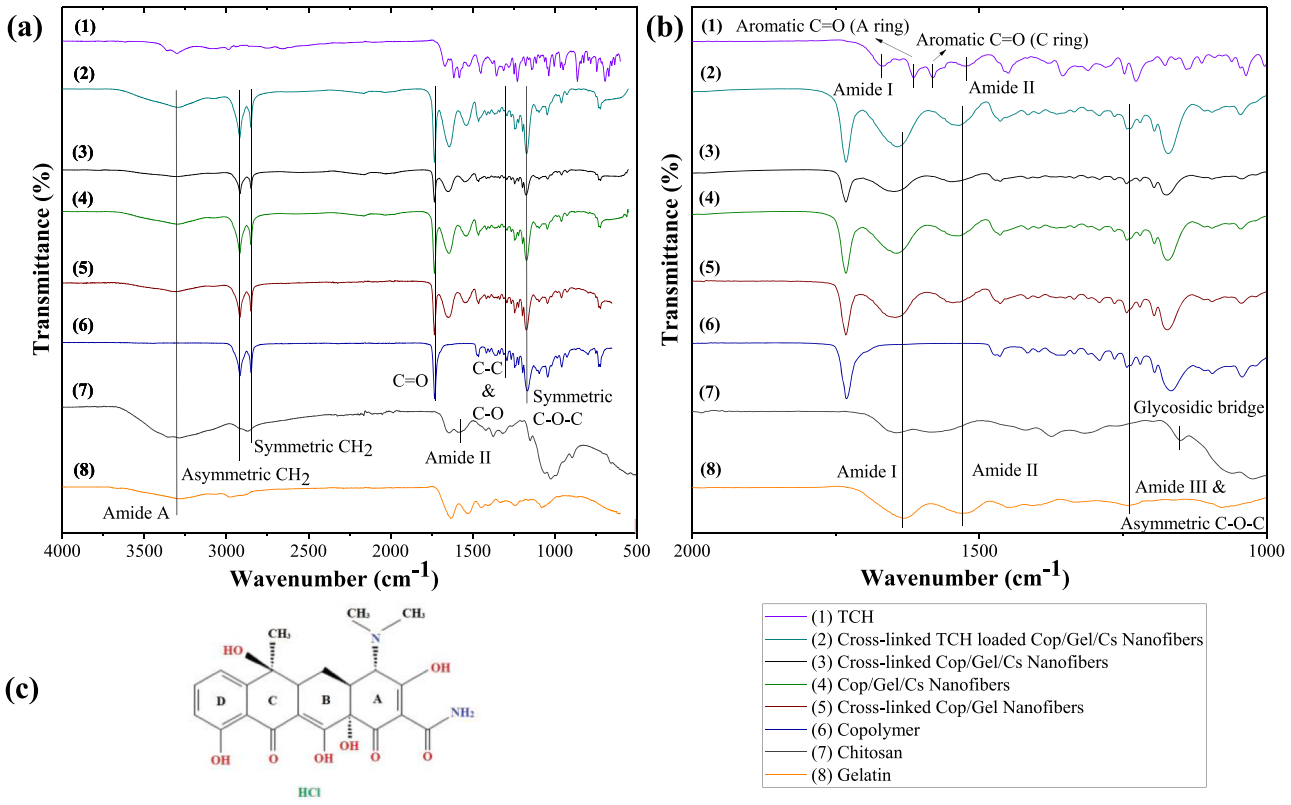

Fig. 7. FTIR spectra of TCH, copolymer, gelatin, chitosan, Cop/Gel/Cs, cross-linked Cop/Gel (Ulker Turan and Guvenilir, 2021), cross-linked neat and 1% TCH-loaded Cop/Gel/Cs nanofibers (a) full spectra, (b) spectra between 2000 and 1000 cm^{-1}, and (c) molecular structure of TCH.

($1293\ cm^{-1}$), asymmetric and symmetric C—O-C stretching ($1245\ cm^{-1}$ and $1167\ cm^{-1}$) were in accordance with literature and detected in spectra of the copolymer and all of its nanofibrous blends (Ulker et al., 2016; Wilberth et al., 2015). In FTIR spectra of all gelatin containing preparations, establishment of characteristic gelatin bands were detected (Spectra 2–5 in Fig. 7). Observed bands associated with gelatin were; N—H stretching vibration at $3302\ cm^{-1}$ (Amide A), C = O stretching and C—NH bending at $1634\ cm^{-1}$ (Amide I), N—H vibration and C—H stretching at $1529\ cm^{-1}$ (Amide II), and C—N bending vibration at $1239\ cm^{-1}$ (Amide III) (Nguyen and Lee, 2010; Zhan et al., 2016a). FTIR spectrum of chitosan exhibited a broad band centered in the region $3289–352\ cm^{-1}$ related to N—H and O—H stretching (Gautam et al., 2014; Liverani et al., 2018; Queiroz et al., 2015; Siqueira et al., 2015; Van Der Schueren et al., 2012). Since this band is common for both gelatin and chitosan, it was observed in spectra of all nanofibrous blend preparations. The absorption bands at $2923\ cm^{-1}$ and $2869\ cm^{-1}$ were assigned to asymmetric and symmetric CH_2 stretching, respectively (Queiroz et al., 2015; Sibaja et al., 2015; Siqueira et al., 2015). These bands were also typical for the copolymer and observed in spectra of all nanofibrous blend preparations with a small shift to lower wavelengths (Ulker et al., 2016; Wilberth et al., 2015). The existence of characteristic chitosan peaks which corresponded to amide I ($1646\ cm^{-1}$) and amide II ($1578\ cm^{-1}$), confirmed the presence of N-acetyl groups and were detected at similar regions with gelatin (Gautam et al., 2014; Liverani et al., 2018; Qiao et al., 2017; Queiroz et al., 2015; Sibaja et al., 2015; Siqueira et al., 2015; Van Der Schueren et al., 2012). Thus, no significant difference observed by the addition of chitosan to binary nanofibrous blend of copolymer and gelatin. In chitosan spectrum, the absorption band around $1151\ cm^{-1}$ can be attributed to C—O-C, C—O, and C—OH bending vibrations confirming the presence of glyosidic bridge in the molecular structure of chitosan (Gautam et al., 2014; Queiroz et al., 2015; Siqueira et al., 2015). This peak may be overlapped with absorption band of copolymer at $1167\ cm^{-1}$ that assigned to symmetric C—O-C stretching bonds (Ulker et al., 2016; Wilberth et al., 2015). A decrease in intensity of amide I, amide-II, and amide-III was noticed by the addition of chitosan to binary nanofibrous blend of copolymer and gelatin (Spectra 3 and 5 in Fig. 7). Such reduction in amplitude of amide I band in FTIR spectrum of cross-linked Cop/Gel/Cs nanofibers may be resulted from alterations in secondary structure of gelatin in nanofibrous blend by the participation of chitosan (Fakhreddin Hosseini et al., 2013; Qiao et al., 2017). Also, intensity of spectrum decreased after cross-linking due to the reaction between glutaraldehyde and NH_2 groups in gelatin and chitosan (Spectra 3 and 4 in Fig. 7) (Grkovic et al., 2017; Schiffman and Schauer, 2007).

Molecular structure of TCH consists of three functional groups which are tricarbonylamide, phenolic diketone, and dimethylamino (Fig. 7(c)). Among them, the most characteristic region is tricarbonylamide (A ring) which composed of an amide and two independent carbonyl groups (Myers et al., 1983). The peaks related with this region were detected at $1670\ cm^{-1}$ (Amide I) and $1525\ cm^{-1}$ (Amide II) (Li et al., 2010; Myers et al., 1983). Other characteristic absorption bands marked on TCH spectrum corresponded to aromatic C = O bonds in A ($1615\ cm^{-1}$) and C rings ($1580\ cm^{-1}$) (Myers et al., 1983). Since amide I and amide II bands were common for TCH, gelatin, and chitosan, there were no significant difference between the spectra of neat and drug-loaded samples. Moreover, peaks related to aromatic C = O bonds were not detectable in TCH-loaded Cop/Gel/Cs sample which may be a result of an absorption shift and/or overlapping.

EDS analysis was applied in order to detect the existence of TCH and distribution of fundamental elements in the structure of cross-linked 1% TCH-loaded Cop/Gel/Cs nanofibers. Molecular structure of TCH includes chlorine (Cl) atom which could be considered as unique marker of TCH (Al-Sabha et al., 2017; Chong et al., 2015). EDS spectrum (Fig. 8) confirmed the presence of Cl atom on the surface of nanofibers indicating that TCH loading was successfully achieved. Also, nitrogen (N) peak was detected due to gelatin and chitosan contents. Strong carbon

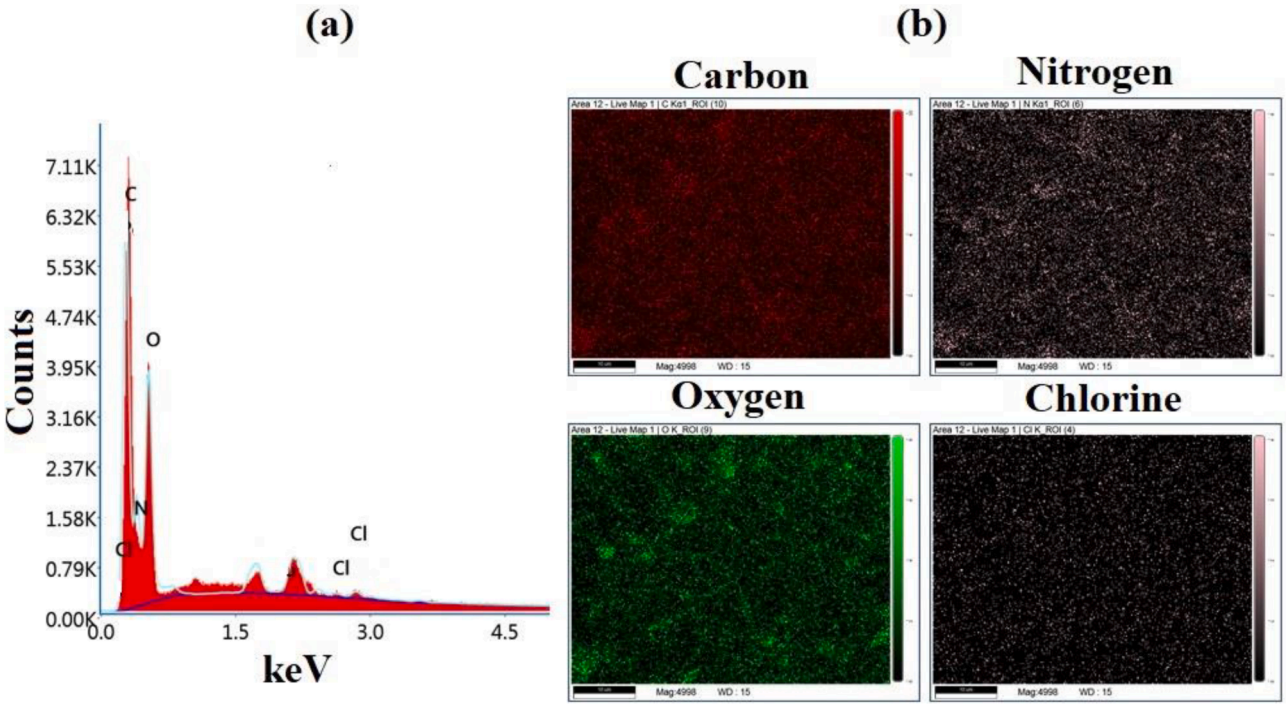

Fig. 8. EDS analysis of cross-linked 1% TCH-loaded Cop/Gel/Cs nanofibrous membrane; (a) Spectrum, (b) Atom distributions.

(C) and oxygen (O) peaks were observed which originated from the backbones of polymers and drug. Fig. 8(b) presents that, C, O, N, and Cl atoms were uniformly distrubuted throughout the surface of the sample as a result of a homogeneous electrospinning process.

3.7. Thermal characterization

Melting temperatures (T_m) of Cop/Gel/Cs, cross-linked neat and 1% TCH-loaded Cop/Gel/Cs nanofibrous membranes were shown on DSC curves (Fig. 9). Also, melting enthalpies (ΔH_m) were calculated from the area under melting peaks of Cop/Gel/Cs, cross-linked neat and TCH-loaded Cop/Gel/Cs nanofibers as 45.5, 80.8, and 53.8 J/g, respectively. Both T_m and ΔH_m values were increased by the cross-linking treatment as a result of enhanced thermal resistance (Nguyen and Lee, 2010; Zhan et al., 2016b).

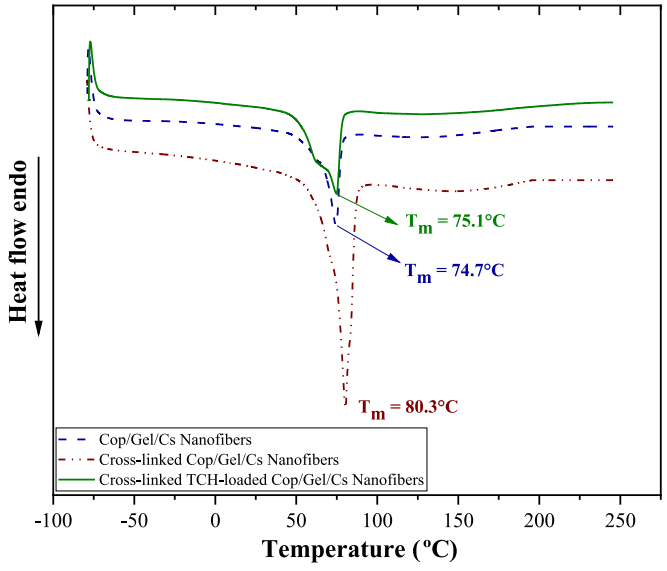

Fig. 9. DSC second heating curves of Cop/Gel/Cs, cross-linked neat and 1% TCH-loaded Cop/Gel/Cs nanofibers.

DSC thermogram of TCH-loaded Cop/Gel/Cs nanofibers did not show endothermic melting peak related to TCH, which is around 220.9 °C (Cervini et al., 2016). The absence of melting peak of TCH indicated that, drug molecule was dispersed in amorphous state without formation of drug crystals within the nanofibrous membrane (He et al., 2017; Shen et al., 2011; Siafaka et al., 2016; Tungprapa et al., 2007; Zamani et al., 2010). An increment was observed in both T_m and ΔH_m values after drug loading, which may be associated with reduction of crystallinity (He et al., 2017; Zamani et al., 2010).

Weight loss (TG) and first derivative of weight loss (DTG) curves of Cop/Gel/Cs, cross-linked neat and 1% TCH-loaded Cop/Gel/Cs nanofibrous membranes were obtained from thermal gravimetric analysis (TGA) and shown in Fig. 10. First mass loss (~5–7%) observed till ~100 °C was common for all samples and related with solvent/moisture evaporation. The degradation pattern, which was detected around ~220 °C in TG and DTG curves of drug-loaded sample, indicates the thermal decomposition of TCH molecule (Cervini et al., 2016). Mass loss around ~320 °C was common for all samples and resulted from primary degradation of gelatin and chitosan (Alavarse et al., 2017; Laha et al., 2016; Nagiah et al., 2013). However, the percentage of degraded part at this step was decreased after cross-linking as a result of increased thermal resistance (Laha et al., 2016; Nagiah et al., 2013). Main degradations due to thermal decomposition of polymeric structure was observed at 404.4 °C, 415.6 °C, and 411.1 °C for Cop/Gel/Cs, cross-linked neat and 1% TCH-loaded Cop/Gel/Cs nanofibrous membranes, respectively. Effect of cross-linking treatment on thermal stability could also be noticed from the increment in main degradation temperatures (Nagiah et al., 2013).

3.8. Antibacterial activity test

Wounds, which occurred on skin due to a cut, surgery or burn, are under the threat of infections caused by bacteria. The majority of skin infections are caused by gram-positive *Staphylococcus* species (*e.g. S. aureus*) which are normally found in skin flora (O'Sullivan et al., 2020;

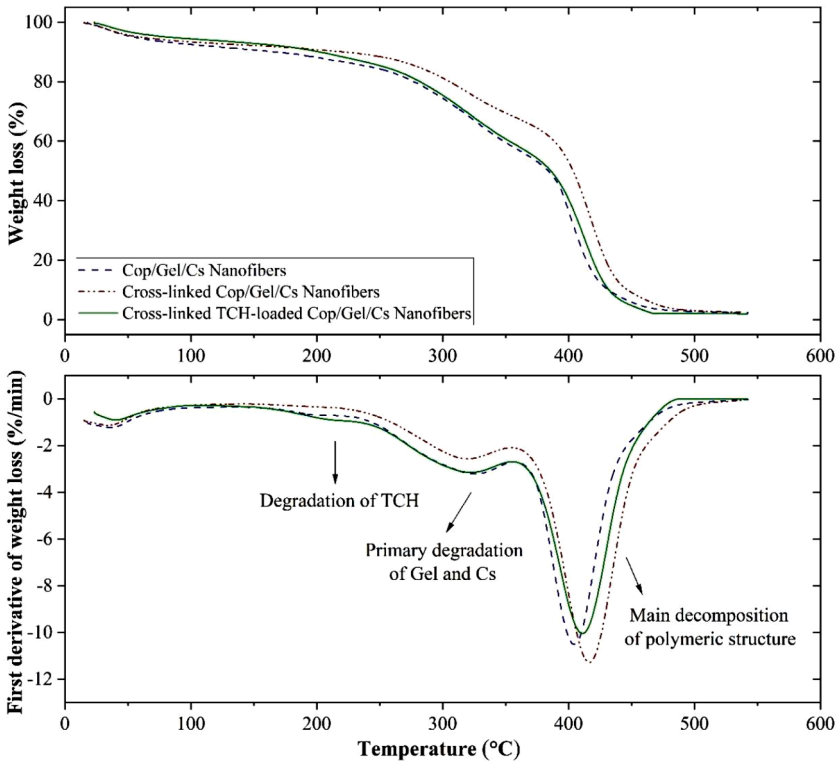

Fig. 10. TGA results of Cop/Gel/Cs, cross-linked neat and 1% TCH-loaded Cop/Gel/Cs nanofibers.

Stulberg et al., 2002). Additionally, gram-negative *E. coli* and gram-positive *B. subtilis* are common bacteria, which could infect the wounds on the skin via contamination from soil, saliva, dirt, or water. Therefore, antibacterial activities of TCH-loaded Cop/Gel/Cs nanofibers (cross-linked) and neat Cop/Gel/Cs (cross-linked) as a negative control (C2) were tested against Gram-positive (*S. aureus* and *B. subtilis*) and Gram-negative (*E. coli*) bacteria by using disk diffusion method, in which bacterial growth inhibition zones are measured (Hudzicki, 2016).

Inhibition zones and their diameters were presented in Fig. 11 and Fig. 12, respectively. All samples with varied antibiotic loading ratios revealed broad and clear inhibition zones (ranged between 14.7 and 27 mm) against *S. aureus* and *B. subtilis*, but antibacterial activity against *E. coli* was limited (~9–10 mm inhibition zone), in fact at 0.5% and 1% TCH loading ratios no inhibition zone was detected. The reason for observation of more efficient antibacterial effect against the Gram-positive *S. aureus* and *B. subtilis* than the Gram-negative *E. coli* is related with difference in their cellular wall structure. *E. coli* bacterium has an additional external cell membrane which is responsible for immune response and may cause antibiotic resistance (Adeli et al., 2019; Alavarse et al., 2017; Oliveira and Reygaert, 2020). Expectedly,

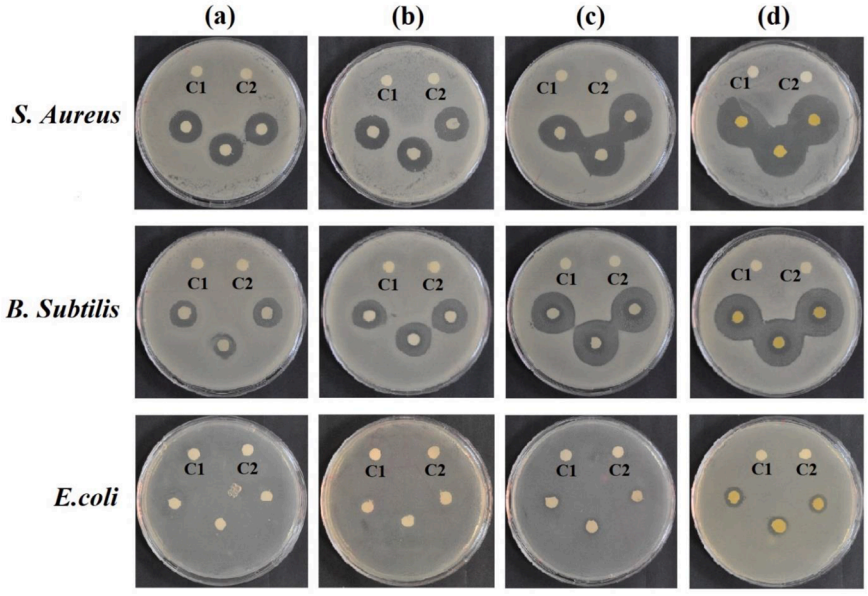

Fig. 11. Antibacterial activities of (a) 0.5%, (b) 1%, (c) 3%, and (d) 5% TCH-loaded Cop/Gel/Cs nanofibrous membranes against *S. aureus, B. Subtilis*, and *E. coli*. Each petri dish includes 5 disks; neat Cop/Gel (C1) and Cop/Gel/Cs (C2) as controls and three replicate samples.

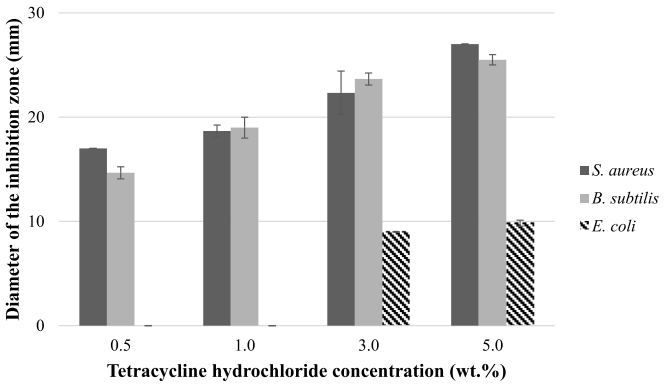

Fig. 12. Inhibition zone diameters.

inhibition zones expanded with increased antibiotic concentration for all types of bacteria. The results revealed that, all drug-loading ratios were appropriate for the treatment of skin wounds caused by gram-positive *S. aureus* and *B. subtilis* bacteria. However, for infections of *E. coli* or to provide a wide spectrum effectiveness, TCH loading ratio of ≥3% would be required.

Chitosan has antibacterial activity, which is due to interruption of the integrity of cell membrane by the interaction of positively charged groups of chitosan and negatively charged cell membrane of bacteria (Adeli et al., 2019; Alavarse et al., 2017; Atay, 2020; Grkovic et al., 2017). Therefore, antibacterial activity of neat Cop/Gel/Cs nanofibrous membranes was compared with neat Cop/Gel (cross-linked) as a negative control (C1) in order to observe if there would be an impact of chitosan addition. However, neat Cop/Gel/Cs nanofibrous membranes did not show a detectable inhibition zone which may be resulted from low chitosan content.

4. Conclusion

In the present study, both neat and TCH-loaded Cop/Gel/Cs electrospun nanofibrous membranes with normally distributed smooth and ultrathin nanofibers were successfully fabricated. SEM images of neat samples showed that, participation of chitosan in nanofibrous structure significantly decreased fiber diameters and 50/40/10 (Cop/Gel/Cs) volume ratio was appropriate to eliminate bead formation resulting to an average fiber diameter of 239.3 nm. Average nanofiber diameters of TCH-loaded preparations were ranged between 85.7–225.2 nm and diameters increased proportional to amount of loaded drug. Expectedly, drug release percentages were higher for low-diameter samples, since they provided high surface area. Based on the drug release experiments, 1% TCH-loaded preparation can be considered as optimal with 96.5% total release and 11.8% initial burst release percentages. By the application of outstanding mathematical models to drug release data, release mechanism was determined as pseudo-Fickian type diffusion. Antibacterial activity test results indicated that, all preparations were effective against Gram-positive bacteria (*S. aureus and B. subtilis*), however preparations with <3% TCH concentration showed no antibacterial activity against Gram-negative *E. coli* bacterium. Therefore, 3% TCH concentration can be suggested as an ideal formulation, at which a wide-spectrum effectiveness can be obtained with a drug release ratio of 61.4%. The presence of gelatin and chitosan made TCH-loaded Cop/Gel/Cs nanofibrous membranes extremely hydrophilic which may provide better contact area with body fluids and enhance drug release. By the use of molecular and thermal characterization methods, appropriate incorporation of drug molecule in the nanofibrous membrane was proved. To conclude based on these results, TCH-loaded poly(ω-pentadecalactone-co-ε-caprolactone)/gelatin/chitosan nanofibrous membranes are suggested to be applied as an antibacterial wound dressing device for treatment of skin infections. This study may provide valuable impacts on literature, since it suggests an application field for an enzymatically synthesized copolymer and brings together a synthetic polymer, a protein, and a polysaccharide by combining their advantages to fabricate an electrospun drug delivery system.

Funding sources

This work has been fully supported by Istanbul Technical University, Scientific Research Projects Coordination Department. Project ID: MDK-2018–41091.

Credit author statement

Cansu Ulker Turan: Investigation, Writing - original draft, Writing - review & editing, Visualization, Formal analysis.
Yuksel Guvenilir: Project administration, Conceptualization, Methodology.

CRediT authorship contribution statement

Cansu Ulker Turan: Investigation, Writing – original draft, Writing – review & editing, Visualization, Formal analysis. **Yuksel Guvenilir:** Project administration, Conceptualization, Methodology.

Declaration of Competing Interest

The authors declare that they have no known competing financial interests or personal relationships that could have appeared to influence the work reported in this paper.

References

Adeli, H., Khorasani, M.T., Parvazinia, M., 2019. Wound dressing based on electrospun PVA/chitosan/starch nanofibrous mats: fabrication, antibacterial and cytocompatibility evaluation and *in vitro* healing assay. Int. J. Biol. Macromol. 122, 238–254. https://doi.org/10.1016/j.ijbiomac.2018.10.115.

Ahmed, S.M., Ahmed, H., Tian, C., Tu, Q., Guo, Y., Wang, J., 2016. Whey protein concentrate doped electrospun poly(epsilon-caprolactone) fibers for antibiotic release improvement. Colloids Surfaces B Biointerfaces 143, 371–381. https://doi.org/10.1016/j.colsurfb.2016.03.059.

Akhmetova, A., Heinz, A., 2021. Electrospinning proteins for wound healing purposes: opportunities and challenges. Pharmaceutics 13, 1–22. https://doi.org/10.3390/pharmaceutics13010004.

Al-Sabha, T.N., Dhamra, M.Y., Al-Ghabsha, T.S., 2017. Spectrofluorimetric Determination of Tetracycline and Terbutaline Sulphate in Its Pure and Dosage Forms Using Eosin Y Reagent. Eur. Chem. Bull. 6, 336. https://doi.org/10.17628/ecb.2017.6.336-342.

Alavarse, A.C., de Oliveira Silva, F.W., Colque, J.T., da Silva, V.M., Prieto, T., Venancio, E.C., Bonvent, J.J., 2017. Tetracycline hydrochloride-loaded electrospun nanofibers mats based on PVA and chitosan for wound dressing. Mater. Sci. Eng. C 77, 271–281. https://doi.org/10.1016/j.msec.2017.03.199.

Albertsson, A.C., Srivastava, R.K., 2008. Recent developments in enzyme-catalyzed ring-opening polymerization. Adv. Drug Deliv. Rev. 60, 1077–1093. https://doi.org/10.1016/j.addr.2008.02.007.

Aldana, A.A., Abraham, G.A., 2017. Current advances in electrospun gelatin-based scaffolds for tissue engineering applications. Int. J. Pharm. 523, 441–453. https://doi.org/10.1016/j.ijpharm.2016.09.044.

Allafchian, A., Hosseini, H., Ghoreishi, S.M., 2020. Electrospinning of PVA-carboxymethyl cellulose nanofibers for flufenamic acid drug delivery. Int. J. Biol. Macromol. 163, 1780–1786. https://doi.org/10.1016/j.ijbiomac.2020.09.129.

Atay, H.Y., 2020. Antibacterial Activity of Chitosan-Based Systems. Functional Chitosan: Drug Delivery and Biomedical Applications.

Augustine, R., Rehman, S.R.U., Ahmed, R., Zahid, A.A., Sharifi, M., Falahati, M., Hasan, A., 2020. Electrospun chitosan membranes containing bioactive and therapeutic agents for enhanced wound healing. Int. J. Biol. Macromol. 156, 153–170. https://doi.org/10.1016/j.ijbiomac.2020.03.207.

Azmana, M., Mahmood, S., Rebhi, A., Rahman, A., Azmir, M., Arifin, B., Ahmed, S., 2021. A review on chitosan and chitosan-based bionanocomposites : promising material for combatting global issues and its applications. Int. J. Biol. Macromol. 185, 832–848. https://doi.org/10.1016/j.ijbiomac.2021.07.023.

Baishya, H., 2017. Application of Mathematical Models in Drug Release Kinetics of Carbidopa and Levodopa ER Tablets. J. Dev. Drugs 06, 1–8. https://doi.org/10.4172/2329-6631.1000171.

Bangar, B., Shinde, N., Deshmukh, S., Kale, B., 2014. Natural polymers in drug delivery development. Res. J. Pharm. Dos. Forms Technol. 6, 54–57.

Basar, A.O., Castro, S., Torres-Giner, S., Lagaron, J.M., Turkoglu Sasmazel, H., 2017. Novel poly(ε-caprolactone)/gelatin wound dressings prepared by emulsion electrospinning with controlled release capacity of Ketoprofen anti-inflammatory drug. Mater. Sci. Eng. C 81, 459–468. https://doi.org/10.1016/j.msec.2017.08.025.

Bhatia, S., 2016. Natural Polymer Drug Delivery Systems: Nanoparticles, Plants, and Algae. Springer International Publishing AG Switzerland. https://doi.org/10.1007/978-3-319-41129-3.

Canbolat, M.F., Celebioglu, A., Uyar, T., 2014. Drug delivery system based on cyclodextrin-naproxen inclusion complex incorporated in electrospun polycaprolactone nanofibers. Colloids Surfaces B Biointerfaces 115, 15–21. https://doi.org/10.1016/j.colsurfb.2013.11.021.

Cervini, P., MacHado, L.C.M., Ferreira, A.P.G., Ambrozini, B., Cavalheiro, É.T.G., 2016. Thermal decomposition of tetracycline and chlortetracycline. J. Anal. Appl. Pyrolysis 118, 317–324. https://doi.org/10.1016/j.jaap.2016.02.015.

Chen, P., Liu, L.-Y., Jiang, Z.-Y., Zheng, .Y..-Y., 2017. The Preparation of core–shell structured gelatin–chitosan nanofibers for biomedical applications. DEStech Trans. Environ. Energy Earth Sci. 2017, 13–17. https://doi.org/10.12783/dteees/edep2017/15516.

Chen, S., Li, R., Li, X., Xie, J., 2018. Electrospinning: an enabling nanotechnology platform for drug delivery and regenerative medicine. Adv. Drug Deliv. Rev. 132, 188–213. https://doi.org/10.1016/j.addr.2018.05.001.

Chong, L.H., Lim, M.M., Sultana, N., 2015. Fabrication and evaluation of polycaprolactone/gelatin-based electrospun nanofibers with antibacterial properties. J. Nanomater. 1–8. https://doi.org/10.1155/2015/970542, 2015.

El-Okaily, M.S., EL-Rafei, A.M., Basha, M., Abdel Ghani, N.T., El-Sayed, M.M.H., Bhaumik, A., Mostafa, A.A., 2021. Efficient drug delivery vehicles of environmentally benign nano-fibers comprising bioactive glass/chitosan/polyvinyl alcohol composites. Int. J. Biol. Macromol. 182, 1582–1589. https://doi.org/10.1016/j.ijbiomac.2021.05.079.

Eskitoros-Togay, M., Bulbul, Y.E., Tort, S., Demirtaş Korkmaz, F., Acartürk, F., Dilsiz, N., 2019. Fabrication of doxycycline-loaded electrospun PCL/PEO membranes for a potential drug delivery system. Int. J. Pharm. 565, 83–94. https://doi.org/10.1016/j.ijpharm.2019.04.073.

Fakhreddin Hosseini, S., Rezaei, M., Zandi, M., Ghavi, F.F., 2013. Preparation and functional properties of fish gelatin-chitosan blend edible films. Food Chem 136, 1490–1495. https://doi.org/10.1016/j.foodchem.2012.09.081.

Gautam, S., Chou, C.F., Dinda, A.K., Potdar, P.D., Mishra, N.C., 2014. Fabrication and characterization of PCL/gelatin/chitosan ternary nanofibrous composite scaffold for tissue engineering applications. J. Mater. Sci. 49, 1076–1089. https://doi.org/10.1007/s10853-013-7785-8.

Ghafoor, B., Aleem, A., Najabat Ali, M., Mir, M., 2018. Review of the fabrication techniques and applications of polymeric electrospun nanofibers for drug delivery systems. J. Drug Deliv. Sci. Technol. 48, 82–87. https://doi.org/10.1016/j.jddst.2018.09.005.

Ghorbani, M., Mahmoodzadeh, F., Yavari Maroufi, L., Nezhad-Mokhtari, P., 2020. Electrospun tetracycline hydrochloride loaded zein/gum tragacanth/poly lactic acid nanofibers for biomedical application. Int. J. Biol. Macromol. 165, 1312–1322. https://doi.org/10.1016/j.ijbiomac.2020.09.225.

Grkovic, M., Stojanovic, D.B., Pavlovic, V.B., Rajilic-Stojanovic, M., Bjelovic, M., Uskokovic, P.S., 2017. Improvement of mechanical properties and antibacterial activity of crosslinked electrospun chitosan/poly (ethylene oxide) nanofibers. Compos. Part B Eng. 121, 58–67. https://doi.org/10.1016/j.compositesb.2017.03.024.

Haroosh, H.J., Dong, Y., Lau, K.T., 2014. Tetracycline hydrochloride (TCH)-loaded drug carrier based on PLA:PCL nanofibre mats: experimental characterisation and release kinetics modelling. J. Mater. Sci. 49, 6270–6281. https://doi.org/10.1007/s10853-014-8352-7.

He, J., Liang, Y., Shi, M., Guo, B., 2020. Anti-oxidant electroactive and antibacterial nanofibrous wound dressings based on poly(ε-caprolactone)/quaternized chitosan-graft-polyaniline for full-thickness skin wound healing. Chem. Eng. J. 385, 123464 https://doi.org/10.1016/j.cej.2019.123464.

He, M., Jiang, H., Wang, R., Xie, Y., Zhao, C., 2017. Fabrication of metronidazole loaded poly (ε-caprolactone)/zein core/shell nanofiber membranes via coaxial electrospinning for guided tissue regeneration. J. Colloid Interface Sci. 490, 270–278. https://doi.org/10.1016/j.jcis.2016.11.062.

Huang, Y., Shi, R., Gong, M., Zhang, J., Li, W., Song, Q., Wu, C., Tian, W., 2018. Icariin-loaded electrospun PCL/gelatin sub-microfiber mat for preventing epidural adhesions after laminectomy. Int. J. Nanomedicine 13, 4831–4844. https://doi.org/10.2147/ijn.s169427.

Hudzicki, J., 2016. Kirby-Bauer Disk Diffusion Susceptibility Test Protocol. Am. Soc. Microbiol. 1–23.

Juncos Bombin, A.D., Dunne, N.J., McCarthy, H.O., 2020. Electrospinning of natural polymers for the production of nanofibres for wound healing applications. Mater. Sci. Eng. C 114, 1–16. https://doi.org/10.1016/j.msec.2020.110994.

Kajdič, S., Planinšek, O., Gašperlin, M., Kocbek, P., 2019. Electrospun nanofibers for customized drug-delivery systems. J. Drug Deliv. Sci. Technol. 51, 672–681. https://doi.org/10.1016/j.jddst.2019.03.038.

Karuppuswamy, P., Reddy Venugopal, J., Navaneethan, B., Luwang Laiva, A., Ramakrishna, S., 2015. Polycaprolactone nanofibers for the controlled release of tetracycline hydrochloride. Mater. Lett. 141, 180–186. https://doi.org/10.1016/j.matlet.2014.11.044.

Kersani, D., Mougin, J., Lopez, M., Degoutin, S., Tabary, N., Cazaux, F., Janus, L., Maton, M., Chai, F., Sobocinski, J., Blanchemain, N., Martel, B., 2020. Stent coating by electrospinning with chitosan/poly-cyclodextrin based nanofibers loaded with simvastatin for restenosis prevention. Eur. J. Pharm. Biopharm. 150, 156–167. https://doi.org/10.1016/j.ejpb.2019.12.017.

Khatti, T., Naderi-Manesh, H., Kalantar, S.M., 2017. Prediction of diameter in blended nanofibers of polycaprolactone-gelatin using ANN and RSM. Fibers Polym. 18, 2368–2378. https://doi.org/10.1007/s12221-017-7631-8.

Kim, K., Luu, Y.K., Chang, C., Fang, D., Hsiao, B.S., Chu, B., Hadjiargyrou, M., 2004. Incorporation and controlled release of a hydrophilic antibiotic using poly(lactide-co-glycolide)-based electrospun nanofibrous scaffolds. J. Control. Release 98, 47–56. https://doi.org/10.1016/j.jconrel.2004.04.009.

Kim, M.S., Kim, G., 2014. Three-dimensional electrospun polycaprolactone (PCL)/alginate hybrid composite scaffolds. Carbohydr. Polym. 114, 213–221. https://doi.org/10.1016/j.carbpol.2014.08.008.

Kumar, M.N.V.R., Domb, A.J., 2008. Drug delivery, controlled. Eds.. In: Wnek, G.E., Bowlin, G.L. (Eds.), Encyclopedia of Biomaterials and Biomedical Engineering. CRC Press, Boca Raton, pp. 880–890. https://doi.org/10.1201/b18990-85.

Laha, A., Yadav, S., Majumdar, S., Sharma, C.S., 2016. In-vitro release study of hydrophobic drug using electrospun cross-linked gelatin nanofibers. Biochem. Eng. J. 105, 481–488. https://doi.org/10.1016/j.bej.2015.11.001.

Li, C., Wang, J., Wang, Yiguang, Gao, H., Wei, G., Huang, Y., Yu, H., Gan, Y., Wang, Yongjun, Mei, L., Chen, H., Hu, H., Zhang, Z., Jin, Y., 2019. Recent progress in drug delivery. Acta Pharm. Sin. B 9, 1145–1162. https://doi.org/10.1016/j.apsb.2019.08.003.

Li, C., Xu, W., Lu, Y., Gross, R.A., 2020. Lipase-Catalyzed Reactive Extrusion: copolymerization of ε-Caprolactone and ω-Pentadecalactone. Macromol. Rapid Commun. 41, 1–7. https://doi.org/10.1002/marc.202000417.

Li, Q., Li, G., Yu, S., Zhang, Z., Ma, F., Feng, Y., 2011. Ring-opening polymerization of ε-caprolactone catalyzed by a novel thermophilic lipase from Fervidobacterium nodosum. Process Biochem 46, 253–257. https://doi.org/10.1016/j.procbio.2010.08.019.

Li, Z., Kolb, V.M.K., Jiang, W.T., Hong, H., 2010. FTIR and XRD investigations of tetracycline intercalation in smectites. Clays Clay Miner 58, 462–474. https://doi.org/10.1346/CCMN.2010.0580402.

Liu, Y., Song, L., Feng, N., Jiang, W., Jin, Y., Li, X., 2020. Recent advances in the synthesis of biodegradable polyesters by sustainable polymerization: lipase-catalyzed polymerization. RSC Adv 10, 36230–36240. https://doi.org/10.1039/d0ra07138b.

Liverani, L., Lacina, J., Roether, J.A., Boccardi, E., Killian, M.S., Schmuki, P., Schubert, D.W., Boccaccini, A.R., 2018. Incorporation of bioactive glass nanoparticles in electrospun PCL/chitosan fibers by using benign solvents. Bioact. Mater. 3, 55–63. https://doi.org/10.1016/j.bioactmat.2017.05.003.

Luong-Van, E., Grøndahl, L., Chua, K.N., Leong, K.W., Nurcombe, V., Cool, S.M., 2006. Controlled release of heparin from poly(??-caprolactone) electrospun fibers. Biomaterials 27, 2042–2050. https://doi.org/10.1016/j.biomaterials.2005.10.028.

Luraghi, A., Peri, F., Moroni, L., 2021. Electrospinning for drug delivery applications: a review. J. Control. Release 334, 463–484. https://doi.org/10.1016/j.jconrel.2021.03.033.

Madhaiyan, K., Sridhar, R., Sundarrajan, S., Venugopal, J.R., Ramakrishna, S., 2013. Vitamin B12 loaded polycaprolactone nanofibers: a novel transdermal route for the water soluble energy supplement delivery. Int. J. Pharm. 444, 70–76. https://doi.org/10.1016/j.ijpharm.2013.01.040.

Martínez-Pérez, C.A., 2020. Electrospinning: a promising technique for drug delivery systems. Rev. Adv. Mater. Sci. 59, 441–454. https://doi.org/10.1515/rams-2020-0041.

Moydeen, A.M., Ali Padusha, M.S., Aboelfetoh, E.F., Al-Deyab, S.S., El-Newehy, M.H., 2018. Fabrication of electrospun poly(vinyl alcohol)/dextran nanofibers via emulsion process as drug delivery system: kinetics and *in vitro* release study. Int. J. Biol. Macromol. 116, 1250–1259. https://doi.org/10.1016/j.ijbiomac.2018.05.130.

Myers, H.M., Tochon-Danguy, H.J., Baud, C.A., 1983. IR absorption spectrophotometric analysis of the complex formed by tetracycline and synthetic hydroxyapatite. Calcif. Tissue Int. 35, 745–749. https://doi.org/10.1007/BF02405117.

Nagiah, N., Madhavi, L., Anitha, R., Srinivasan, N.T., Sivagnanam, U.T., 2013. Electrospinning of poly (3-hydroxybutyric acid) and gelatin blended thin films: fabrication, characterization, and application in skin regeneration. Polym. Bull. 70, 2337–2358. https://doi.org/10.1007/s00289-013-0956-6.

Nguyen, T.-.H., Lee, .B..-T., 2010. Fabrication and characterization of cross-linked gelatin electro-spun nano-fibers. J. Biomed. Sci. Eng. 03, 1117–1124. https://doi.org/10.4236/jbise.2010.312145.

O'Sullivan, J.N., Rea, M.C., Hill, C., Ross, R.P., 2020. Protecting the outside: biological tools to manipulate the skin microbiota. FEMS Microbiol. Ecol. 96, 1–14. https://doi.org/10.1093/femsec/fiaa085.

Oliveira, J., Reygaert, W.C., 2020. Gram Negative Bacteria. StatPearls [Internet]. StatPearls Publishing, Treasure Island (FL).

Pelipenko, J., Kocbek, P., Kristl, J., 2015. Critical attributes of nanofibers: preparation, drug loading, and tissue regeneration. Int. J. Pharm. 484, 57–74. https://doi.org/10.1016/j.ijpharm.2015.02.043.

Peppas, N.A., 1985. Analysis of Fickian and non-Fickian drug release from polymers. Pharm. Acta Helv. 60, 110–111.

Pereira, I.H.L., Ayres, E., Averous, L., Schlatter, G., Hebraud, A., De Paula, A.C.C., Viana, P.H.L., Goes, A.M., Oréfice, R.L., 2014. Differentiation of human adipose-derived stem cells seeded on mineralized electrospun co-axial poly(ε-caprolactone) (PCL)/gelatin nanofibers. J. Mater. Sci. Mater. Med. 25, 1137–1148. https://doi.org/10.1007/s10856-013-5133-9.

Pisani, S., Dorati, R., Chiesa, E., Genta, I., Modena, T., Bruni, G., Grisoli, P., Conti, B., 2019. Release Profile of Gentamicin Sulfate from Polylactide-co-Polycaprolactone Electrospun Nanofiber Matrices. Pharmaceutics 11, 1–14. https://doi.org/10.3390/pharmaceutics11040161.

Qasim, S.B., Zafar, M.S., Najeeb, S., Khurshid, Z., Shah, A.H., Husain, S., Rehman, I.U., 2018. Electrospinning of chitosan-based solutions for tissue engineering and

regenerative medicine. Int. J. Mol. Sci. 19, 1–26. https://doi.org/10.3390/ijms19020407.
Qiao, C., Ma, X., Zhang, J., Yao, J., 2017. Molecular interactions in gelatin/chitosan composite films. Food Chem 235, 45–50. https://doi.org/10.1016/j.foodchem.2017.05.045.
Queiroz, M.F., Melo, K.R.T., Sabry, D.A., Sassaki, G.L., Rocha, H.A.O., 2015. Does the use of chitosan contribute to oxalate kidney stone formation? Mar. Drugs 13, 141–158. https://doi.org/10.3390/md13010141.
Radisavljevic, A., Stojanovic, D.B., Perisic, S., Djokic, V., Radojevic, V., Rajilic-Stojanovic, M., Uskokovic, P.S., 2018. Cefazolin-loaded polycaprolactone fibers produced via different electrospinning methods: characterization, drug release and antibacterial effect. Eur. J. Pharm. Sci. 124, 26–36. https://doi.org/10.1016/j.ejps.2018.08.023.
Samrot, A.V., Sean, T.C., Kudaiyappan, T., Bisyarah, U., Mirarmandi, A., Faradjeva, E., Abubakar, A., Ali, H.H., Angalene, J.L.A., Suresh Kumar, S., 2020. Production, characterization and application of nanocarriers made of polysaccharides, proteins, bio-polyesters and other biopolymers: a review. Int. J. Biol. Macromol. 165, 3088–3105. https://doi.org/10.1016/j.ijbiomac.2020.10.104.
Saurí, J., Millán, D., Suñé-Negre, J.M., Colom, H., Ticó, J.R., Miñarro, M., Pérez-Lozano, P., García-Montoya, E., 2014. Quality by design approach to understand the physicochemical phenomena involved in controlled release of captopril SR matrix tablets. Int. J. Pharm. 477, 431–441. https://doi.org/10.1016/j.ijpharm.2014.10.050.
Schiffman, J.D., Schauer, C.L., 2007. Cross-linking chitosan nanofibers. Biomacromolecules 8, 594–601. https://doi.org/10.1021/bm060804s.
Shah, K.U., Khan, G.M., 2012. Regulating drug release behavior and kinetics from matrix tablets based on fine particle-sized ethyl cellulose ether derivatives: an *in vitro* and *in vivo* evaluation. Sci. World J. 2012, 1–8. https://doi.org/10.1100/2012/842348.
Shen, X., Yu, D., Zhu, L., Branford-White, C., White, K., Chatterton, N.P., 2011. Electrospun diclofenac sodium loaded Eudragit® L 100-55 nanofibers for colon-targeted drug delivery. Int. J. Pharm. 408, 200–207. https://doi.org/10.1016/j.ijpharm.2011.01.058.
Siafaka, P.I., Barmbalexis, P., Bikiaris, D.N., 2016. Novel electrospun nanofibrous matrices prepared from poly(lactic acid)/poly(butylene adipate) blends for controlled release formulations of an anti-rheumatoid agent. Eur. J. Pharm. Sci. 88, 12–25. https://doi.org/10.1016/j.ejps.2016.03.021.
Sibaja, B., Culbertson, E., Marshall, P., Boy, R., Broughton, R.M., Solano, A.A., Esquivel, M., Parker, J., Fuente, L.D.La, Auad, M.L., 2015. Preparation of alginate-chitosan fibers with potential biomedical applications. Carbohydr. Polym. 134, 598–608. https://doi.org/10.1016/j.carbpol.2015.07.076.
Sill, T.J., von Recum, H.A., 2008. Electrospinning: applications in drug delivery and tissue engineering. Biomaterials 29, 1989–2006. https://doi.org/10.1016/j.biomaterials.2008.01.011.
Siqueira, N.M., Garcia, K.C., Bussamara, R., Both, F.S., Vainstein, M.H., Soares, R.M.D., 2015. Poly (lactic acid)/chitosan fiber mats: investigation of effects of the support on lipase immobilization. Int. J. Biol. Macromol. 72, 998–1004. https://doi.org/10.1016/j.ijbiomac.2014.08.048.
Sofi, H.S., Abdal-hay, A., Ivanovski, S., Zhang, Y.S., Sheikh, F.A., 2020. Electrospun nanofibers for the delivery of active drugs through nasal, oral and vaginal mucosa: current status and future perspectives. Mater. Sci. Eng. C 111, 110756. https://doi.org/10.1016/j.msec.2020.110756.
Sridhar, R., Lakshminarayanan, R., Madhaiyan, K., Barathi, V.A., Limh, K.H.C., Ramakrishna, S., 2015. Electrosprayed nanoparticles and electrospun nanofibers based on natural materials: applications in tissue regeneration, drug delivery and pharmaceuticals. Chem. Soc. Rev. 44, 790–814. https://doi.org/10.1039/c4cs00226a.
Stulberg, D.L., Penrod, M.A., Blatny, R.A., 2002. Common bacterial skin infections. Am. Fam. Physician 66, 119–124. https://doi.org/10.1080/00325481.1993.11701692.
Topuz, F., Uyar, T., 2019. Electrospinning of cyclodextrin functional nanofibers for drug delivery applications. Pharmaceutics 11, 1–35. https://doi.org/10.3390/pharmaceutics11010006.
Torres-Martinez, E.J., Cornejo Bravo, J.M., Serrano Medina, A., Pérez González, G.L., Villarreal Gómez, L.J., 2018. A summary of electrospun nanofibers as drug delivery system: drugs loaded and biopolymers used as matrices. Curr. Drug Deliv. 15, 1360–1374. https://doi.org/10.2174/1567201815666180723114326.
Tungprapa, S., Jangchud, I., Supaphol, P., 2007. Release characteristics of four model drugs from drug-loaded electrospun cellulose acetate fiber mats. Polymer (Guildf) 48, 5030–5041. https://doi.org/10.1016/j.polymer.2007.06.061.
Ulker, C., Gokalp, N., Guvenilir, Y., 2016. Enzymatic synthesis and characterization of polycaprolactone by using immobilized lipase onto a surface-modified renewable carrier. Polish J. Chem. Technol. 18, 134–140.
Ulker, C., Guvenilir, Y., 2018. Enzymatic synthesis and characterization of biodegradable poly(w-pentadecalactone-co-e-caprolactone) copolymers. J. Renew. Mater. 6, 591–598. https://doi.org/10.7569/JRM.2017.634189.
Ulker Turan, C., Guvenilir, Y., 2021. Fabrication and characterization of electrospun biopolyester/gelatin nanofibers. J. Biomed. Mater. Res. - Part B Appl. Biomater. 1–10. https://doi.org/10.1002/jbm.b.34807.
Ulker Turan, C., Metin, A., Guvenilir, Y., 2021. Controlled release of tetracycline hydrochloride from poly(ω-pentadecalactone-co-ε-caprolactone)/gelatin nanofibers. Eur. J. Pharm. Biopharm. 162, 59–69. https://doi.org/10.1016/j.ejpb.2021.02.009.
Van Der Schueren, L., Steyaert, I., De Schoenmaker, B., De Clerck, K., 2012. Polycaprolactone/chitosan blend nanofibres electrospun from an acetic acid/formic acid solvent system. Carbohydr. Polym. 88, 1221–1226. https://doi.org/10.1016/j.carbpol.2012.01.085.
Wilberth, H.K., Manuel, C.U.J., Tania, L.C., Manuel, A.V., 2015. Effect of reaction temperature on the physicochemical properties of poly(pentadecanolide) obtained by enzyme-catalyzed ring-opening polymerization. Polym. Bull. 72, 441–452. https://doi.org/10.1007/s00289-014-1288-x.
Yang, S., Zhang, X., Zhang, D., 2019. Electrospun chitosan/poly (vinyl alcohol)/graphene oxide nanofibrous membrane with ciprofloxacin antibiotic drug for potential wound dressing application. Int. J. Mol. Sci. 20 https://doi.org/10.3390/ijms20184395.
Ye, K., Kuang, H., You, Z., Morsi, Y., Mo, X., 2019. Electrospun nanofibers for tissue engineering with drug loading and release. Pharmaceutics 11, 1–17. https://doi.org/10.3390/pharmaceutics11040182.
Zamani, M., Morshed, M., Varshosaz, J., Jannesari, M., 2010. Controlled release of metronidazole benzoate from poly ε-caprolactone electrospun nanofibers for periodontal diseases. Eur. J. Pharm. Biopharm. 75, 179–185. https://doi.org/10.1016/j.ejpb.2010.02.002.
Zhan, J., Morsi, Y., Ei-Hamshary, H., Al-Deyab, S.S., Mo, X., 2016a. *In vitro* evaluation of electrospun gelatin–glutaraldehyde nanofibers. Front. Mater. Sci. 10, 90–100. https://doi.org/10.1007/s11706-016-0329-9.
Zhan, J., Morsi, Y., Hamshary, H.E.I., Deyab, S.S.A.L., Mo, X., 2016b. *In vitro* evaluation of electrospun gelatin – glutaraldehyde nanofibers 10, 90–100. https://doi.org/10.1007/s11706-016-0329-9.
Zhang, Y.Z., Venugopal, J., Huang, Z.M., Lim, C.T., Ramakrishna, S., 2006. Crosslinking of the electrospun gelatin nanofibers. Polymer (Guildf). 47, 2911–2917. https://doi.org/10.1016/j.polymer.2006.02.046.